Graphene/phosphorene bilayer: High electron speed, optical property and semiconductor-metal transition with electric field

CrossMark

Arqum Hashmi, Umar Farooq, Jisang Hong*

Department of Physics, Pukyong National University, Busan 608-737, South Korea

A B S T R A C T

We investigated the electric field dependent band structures and optical properties of graphene/phosphorene bilayer. Remarkably, the effective electron Fermi velocity in graphene/phosphorene was comparable to that of pure graphene monolayer. Moreover, this feature was not disrupted even in the presence of a finite external electric field. The electronic band structure changed from a semiconductor to a metallic state with an external electric field strength of 0.5 V/Å. In addition, the electric field enhanced the structural stability of a bilayer system because the binding energy was increased approximately 20 −30% as compared with that at zero electric field. We found that the optical anisotropy regarding the electric polarization along armchair and zigzag directions disappeared, but the anisotropic optical properties still survived regarding the electric polarization for in-plane and perpendicular directions. The small effective mass, high speed of electrons, and optical property in graphene/phosphorene bilayer may provide a promising way for graphene based device applications.

© 2015 Elsevier B.V. All rights reserved.

1. Introduction

Recently, a new 2D material phosphorene named after its parent black phosphorus was mechanically exfoliated by scotch tape based microcleavage method from layered bulk black phosphorus [1–3]. Comparing with the graphene, the most striking difference is that the phosphorene has a direct band gap, whereas the graphene shows a zero gap at K-point. Due to this semiconducting feature, the phosphorene may be superior to the graphene for device applications in many ways. Along with the band gap, interestingly, few layer black phosphorene based field effect transistors have high mobility and high on/off ratio [1,4]. Besides, it exhibits anisotropic optical, mechanical and electron transport properties [2,5–7]. For instance, the frequency dependent dielectric functions along armchair and zigzag directions display substantially different spectral shapes. No such anisotropic behavior has been found in any other 2D layer structured materials. In geometric point of view, the phosphorene layer has also a peculiar feature because it shows a puckered layer geometry. It seems that the geometric feature induces the anisotropy in transport as well as in optical properties. Due to these optical and transport properties, we expect that the phosphorene may open next-generation devices applications.

Both graphene and phosphorene have their own unique physical properties, and the study on phosphorene is now becoming an emerging field. Thus, it will be of particular interest to explore the physical properties of graphene/phosphorene hybridized bilayer system. Recently, Padilha et al. studied the graphene/phosphorene bilayer system to control the schottky barrier height as well as the doping of phosphorene [8]. Consequently, from the perspective of high speed nano devices, it will be very important to study the effective mass, effective electron Fermi velocity, and optical properties of graphene/phosphorene hybridized bilayer system. In this report, we aim to investigate the following issues: (i) stability of bilayer system and interaction type between two layers (ii) band dispersion and effective mass in graphene/phosphorene (iii) optical properties. In addition, we explore the electric field dependence of those properties.

2. Numerical method

We performed all the calculations using the Vienna ab initio simulation package (VASP) [9,10]. Valence electrons were treated explicitly and their interactions with ionic cores were described by projector augmented wave (PAW) pseudopotentials [11]. We explored the structural, adsorption and electronic properties of graphene/phosphorene bilayer structure using a non-empirical

* Corresponding author.
  E-mail address: hongj@pknu.ac.kr (J. Hong).

vdW-DF method proposed by Dion et al. [12] We used most recently developed less repulsive optB88-like exchange functional [13] because this new functional showed significant improvement in binding energies and interlayer distances [12,14,15]. All results reported here were obtained with high plane-wave energy cut-off 600 eV. The Brillouin-zone integration was performed using the Monkhorst-Pack k-point sampling with a $6 \times 18 \times 1$ k-mesh. In particular, we used 600 k-points to obtain an accurate energy gap at the Dirac point. To simulate the graphene/phosphorene bilayer, we employed (5×1) phosphorene supercell and (4×2) graphene supercell. In our calculations, we considered two systems; (i) bilayer with graphene lattice constant and (ii) bilayer with phosphorene lattice constant. In both cases, we fully allowed structure relaxation without any constraint and compared the total energies. We found that the bilayer with graphene lattice constant was more stable by 4 eV than phosphorene lattice constant. As a result, we used the graphene lattice constant. Consequently, the overall strain in the phosphorene lattice was less than 2%. Both layers were fully relaxed with graphene lattice constant until the energy and forces are less than 0.1 meV and 0.01 eVA^{-1}, respectively. We imposed a vacuum region of 15 A in the z direction. Charge analysis to calculate the electron transfer between the graphene and the phosphorene layers was performed using Bader formalism [16,17]. To calculate the optical properties of phosphorene/graphene nanocomposite, the frequency-dependent dielectric matrix is calculated using PAW potentials. The imaginary part is determined by a summation over empty states using the equation [18].

$$\varepsilon''_{\alpha\beta}(\omega) = \frac{4\pi^2 e^2}{\Omega} \lim_{q \to 0} \frac{1}{q^2} \sum_{c,v,k} 2\omega_k \delta(\varepsilon_{ck} - \varepsilon_{vk} - \omega)$$
$$\times \ \mu_{ck+e_{\alpha q}} |\mu_{vk} \mu_{ck+e_{\alpha q}}| \mu^*_{vk} \qquad (1)$$

where the indices c and v represent conduction and valence band states, respectively, and μ_{ck} refers to the cell periodic part of the orbitals at the k point. A large number of empty conduction band states (two times more than the number of valence band) are included for the summation in equation.

3. Numerical results

Fig. 1 (a) and (b) shows a schematic illustration of the side and top views. The graphene layer preserved its original flat plane structure and also the bond length. In contrast, the bond length in phosphorene sheet was considerably changed. Nonetheless, the phosphorene sheet maintained its own puckered layer geometry in heterostructure. We found an interface binding energy of 33 meV per atom, and this value was quite close to the bilayer graphene binding energy [19]. Besides, the interlayer distance between graphene and phosphorene layers was about 3.47 Å and quite agrees with previous report [8]. The interlayer distance between phosphorene and graphene was much larger than the sum of covalent radii of C and P atoms. The calculated binding energy and interlayer distance indicates that the hybridized system has a weak van der Waals interaction. Fig. 2(a) shows the band structure of pristine graphene layer and the zero gap is observed. This may validate our method to calculate the band gap of bilayer system. Fig. 2 (b) shows the three dimensional band structure of bilayer system and we obtained an energy gap of 4 meV. This tiny value can be interpreted as a zero-gap and the gap is originated from the graphene layer. Interestingly, the linearity in band dispersion of graphene was not disrupted even in the presence of a phosphorene layer. This is the same thing found in graphene/BN bilayer system with finite bandgap [20]. On the other hand, we found no significant modification in the phosphorene band structure as
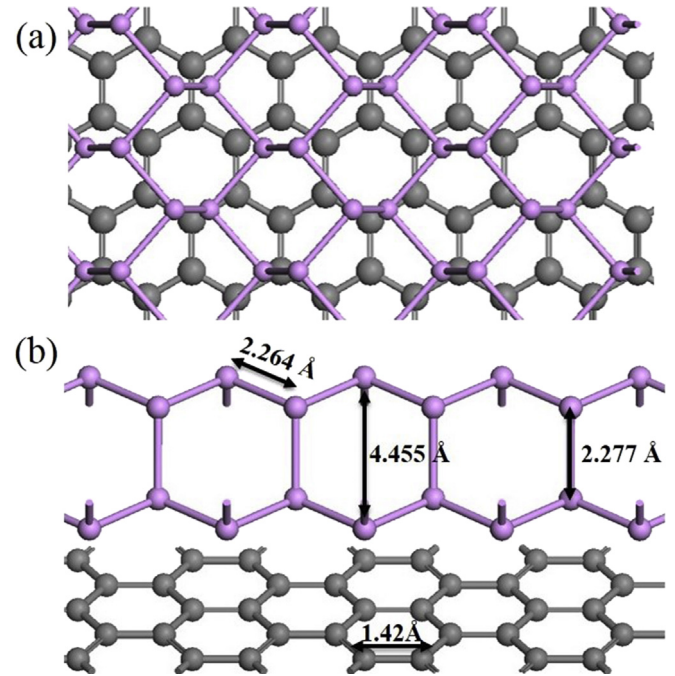

Fig. 1. (a) side and (b) top view of the fully relaxed bilayer graphene/phosphorene heterostructure. Bond lengths of optimized bilayer graphene/phosphorene is shown in figure. Pink and gray balls represent P and C atoms, respectively. (For interpretation of the references to colour in this figure legend, the reader is referred to the web version of this article.)

compared with that of a free standing phosphorene layer. In Fig. 2 (c) and (d), we presented the partial density of states (PDOS). It is clearly shown that the negligible gap in graphene originates from p_z orbital of a carbon atom. In addition, the p_z orbital of the phosphorus atom contributed to the gap in the phosphorene layer. We also investigated the electron coupling at the graphene/phosphorene interface. To observe the intensity of electron cloud overlap, we plotted the total charge density of the bilayer with an iso-surface value of 0.11 e/Å^3 in Fig. 2 (e). The electron cloud on the graphene plane mostly distributed on C–C bonds while the electron cloud on the phosphorene layer mostly existed between phosphorus atoms in a puckered geometry. We found no meaningful electron cloud overlap between the phosphorene and π-electron of graphene. This well agrees with our conclusion that the bilayer has a weak van der Waals interaction. To investigate charge transfer between two layers, we calculated the difference in charge density and performed Bader charge analysis. Fig 2 (f) shows the charge density difference with an iso-surface value of 0.0002 e/Å^3. Overall, the interaction between two layers was rather weak due to the relatively large interlayer distance, and the Bader charge analysis showed that there is no change transfer between two layers.

To study the external electric field effect on the electronic structure, we applied the electric field (E-field) perpendicular to the plane of graphene/phosphorene bilayer. Electric field is introduced by adding an artificial dipole sheet in the middle of the vacuum part in the periodic supercell [21]. The E-field intensity was changed from −0.5 to 0.5 V/Å. Here, we considered both positive (from graphene to phosphorene: +z direction) and negative (from phosphorene to graphene:-z direction) E-filed directions. At zero external electric field, the energy gap was equivalent to the energy difference between upper and lower Dirac cones. Thus, we calculated this difference at a finite external electric field. Besides, the electric field dependent binding energy was also investigated. Fig. 3